3.8-mm penetration on the first attempt and a 4.1-mm penetration on the second attempt. The brushing and grinding operations on Mazatzal showed the presence of a dark, smooth, indurated coating beneath the light-toned loose coating (Fig. 3). This dark coating was largely removed by the second grinding, revealing the underlying rock surface (Fig. 3B). There is also some evidence that a second bright coating may underlie the dark coating (*10*, *11*).

Grind motor currents, the depths achieved, and grinding areas provided estimates of the amount of energy consumed by the RAT while removing a unit volume of material. Because grind energy density is a nontraditional means of quantifying rock mechanical properties, three terrestrial rocks were abraded in the laboratory for calibration, with the use of a flight-like RAT: a fresh, nonvesicular basalt sample from Ash Fork, Arizona; a fine-grained dolostone sample collected from the Soda Mountains north of Silver Lake, California; and Cleveland Member (fissle shale) of the Ohio Formation. These experiments yielded energy densities of ~166, 83, and 11 J/mm^3, respectively. For comparison, Humphrey required 83 J/mm^3, whereas Adirondack and Mazatzal required 51 and 65 J/mm^3, respectively. Thus, rocks abraded by Spirit required less energy per volume than the particular basalt sample ground in the tests, and comparable grind energy densities to the two terrestrial sedimentary rock samples, even though composition and mineralogy data from Spirit demonstrate that the rocks encountered are basalts (*10*, *12*–*14*).

The physical properties experiments conducted by Spirit at Gusev crater show that surface soils are cloddy, rock coatings are ubiquitous, and rocks are easily abraded and thus mechanically weaker than the fresh, nonvesicular basaltic sample used in the laboratory tests. Furthermore, the abraded surfaces of the rocks at Gusev exposed vugs and cracks filled with bright material suggestive of aqueous mineralization (Fig. 3) (*10*, *11*). There is also a suggestion of a vertical weathering profile for Humphrey rock, where the grinding direction was accomplished at a slight angle from the surface normal, thereby exposing shallow to deep surfaces (*10*). The presence of liquid water, even for brief periods of time, is one way to cement surface soils, form rock coatings, deposit minerals in vugs and cracks, and weather the surfaces of rocks. Liquid water might occur for brief periods when the spin axis obliquity and atmospheric relative humidity are high and precipitation occurs as snow or frost (*15*). A modest temperature enhancement as a result of absorption of solar radiation by underlying regolith and rocks, with "greenhouse"-related absorption of outgoing thermal radiation by the ice and snow, could generate thin films of liquid water that would mobilize soluble species and produce the features observed by Spirit. Other models are also being explored to place the physical properties experiments in an environmental context, in addition to further measurements designed to test hypotheses.

References and Notes

1. A martian solar day has a mean period of 24 hours 39 min 35.244 s and is referred to as a sol to distinguish this from a roughly 3% shorter solar day on Earth. A martian sidereal day, as measured with respect to the fixed stars, is 24 hours 37 min 22.663 s, as compared with 23 hours 56 min 04.0905 s for Earth. See www.giss.nasa.gov/tools/mars24 for more information.
2. Names have been assigned to areographic features by the Mars Exploration Rover (MER) team for planning and operations purposes. The names are not formally recognized by the IAU.
3. J. A. Grant *et al.*, *Science* **305**, 807 (2004).
4. The term martian soil is used here to denote any loose unconsolidated materials that can be distinguished from rocks, bedrock, or strongly cohesive sediments. No implication of the presence or absence of organic materials or living matter is intended.
5. P. R. Christensen *et al.*, *Science* **305**, 837 (2004).
6. R. Greeley *et al.*, *Science* **305**, 810 (2004).
7. G. Landis, P. Jenkins, *J. Geophys. Res.* **105**, 1855 (2000).
8. Based on wheel track sinkage values for terrains covered by one to three MER wheels described in L. Richter and P. Hamacher, paper presented at the 13th Conference of the International Society for Terrain-Vehicle Systems, Munich, Germany, 14 to 17 September 1999.
9. H. Moore *et al.*, *J. Geophys. Res.* **104**, 8729 (1999).
10. K. E. Herkenhoff *et al.*, *Science* **305**, 824 (2004).
11. H. Y. McSween *et al.*, *Science* **305**, 842 (2004).
12. S. W. Squyres *et al.*, *Science* **305**, 794 (2004).
13. J. F. Bell III *et al.*, *Science* **305**, 800 (2004).
14. P. R. Christensen *et al.*, *Science* **305**, 837 (2004).
15. M. A. Mischna *et al.*, *J. Geophys. Res.* **108**, 5062 (2003).
16. Work funded by NASA through the Mars Exploration Rover Project. We thank the MER team of scientists and engineers, who made the landing, traverses, and science observations a reality.

4 May 2004; accepted 2 July 2004

REPORT

Textures of the Soils and Rocks at Gusev Crater from Spirit's Microscopic Imager

K. E. Herkenhoff,[1]* S. W. Squyres,[2] R. Arvidson,[3] D. S. Bass,[4] J. F. Bell III,[2] P. Bertelsen,[5] N. A. Cabrol,[6] L. Gaddis,[1] A. G. Hayes,[2] S. F. Hviid,[7] J. R. Johnson,[1] K. M. Kinch,[8] M. B. Madsen,[5] J. N. Maki,[4] S. M. McLennan,[9] H. Y. McSween,[10] J. W. Rice Jr.,[11] M. Sims,[12] P. H. Smith,[13] L. A. Soderblom,[1] N. Spanovich,[13] R. Sullivan,[2] A. Wang[14]

The Microscopic Imager on the Spirit rover analyzed the textures of the soil and rocks at Gusev crater on Mars at a resolution of 100 micrometers. Weakly bound agglomerates of dust are present in the soil near the Columbia Memorial Station. Some of the brushed or abraded rock surfaces show igneous textures and evidence for alteration rinds, coatings, and veins consistent with secondary mineralization. The rock textures are consistent with a volcanic origin and subsequent alteration and/or weathering by impact events, wind, and possibly water.

The Microscopic Imager (MI) is a fixed-focus camera mounted on a robotic arm (*1*, *2*). The MI was designed to function like a geologist's hand lens, acquiring images at a spatial resolution of 31 μm/pixel (picture element) over a broad spectral range (400 to 700 nm). The MI uses the same electronics design as the other Mars Exploration Rover (MER) cameras (*3*, *4*), but its optics yield a field of view of 32 by 32 mm across a 1024- by 1024-pixel charge-coupled device image. The MI acquires images with only solar or skylight illumination of the target surface. A contact sensor is used to place the MI slightly closer to the target surface than its best-focus distance of about 66 mm, which allows concave surfaces to be imaged in good focus. The depth of field of the MI is ~3 mm; coarse focusing (~2-mm precision) is achieved by moving the arm away from a rock target after contact is sensed. The MI optics are protected from the martian environment by a retractable dust cover. This cover includes a Kapton (polyimide film, DuPont, Wilmington, Delaware) window that is tinted orange to restrict the spectral bandpass to 500 to 700 nm, which allows crude color information to be obtained by acquiring images with the cover open and closed.

During the first 90 sols (*5*), Spirit acquired and returned 537 MI images of seven rocks, many martian soil (*6*) and bedform targets, and the martian sky (for calibration). Tracks and trenches created by the rover wheels were also imaged (*7*), as were the filter and capture magnets on the front of the rover (*8*).

As part of the daily MER operations process (*9*), targets for the MI and other arm instruments were selected by using available Pancam (*10*), Navcam, and Hazcam imagery (*4*). The MI routinely observed targets that were investigated by the other ARM instruments to study surface details, to provide context for the spectrometer data, and to examine the results of rock abrasion tool (RAT) brushing and grinding activities (*2*, *11*, *12*, *13*). Many of the Mössbauer spectrometer (*11*) soil targets were imaged twice by the MI (before and after Mössbauer touch) to observe the physical effects of the Mössbauer contact sensor on the soil and to determine the location of the Mössbauer field of view.

A typical MI data set includes a stack of three, five, or seven MI images, acquired at 3-mm steps along the MI optical axis with the dust cover open (*1*). This acquisition approach helped to ensure optimum focus on targets with relief greater than the MI depth of field. The number of images in an MI stack was kept small to minimize the volume of extraneous MI data returned to Earth. Most of the MI stacks included at least one image in good focus, but uncertainties in the front Hazcam terrain model resulted in poorly focused MI images in some cases. Color information was sometimes added by acquiring an additional single-frame MI image of the same target at the nominal best-focus position with the dust cover closed. Some of the MI targets were imaged with a binocular stereo pair of left/right MI stacks or even a mosaic of MI stacks (e.g., Plates 12 and 13).

Soil materials at Gusev that have been examined by the MI show texture down to the limit of resolution, about 100 μm (*14*). Soil surfaces typically are rough at submillimeter scales but are molded to much smoother surfaces under compression by the Mössbauer contact plate and/or a rover wheel, revealing the presence of a substantial fraction of particles too small to be resolved. It is unclear how much remolding was accomplished by compression of void space and reorganization of existing particles, or by destruction of weak particles to even smaller sizes. Soil texture was obliterated by the ~1 N force applied by the Mössbauer contact plate (Fig. 1). If this was due to crushing of particles, the original particles must have been very weak. Some soils preserve a vertically coherent network (100 to 300 μm scale) of tubelike and honeycomb features. These observations are con-

[1]U.S. Geological Survey Astrogeology Team, Flagstaff, AZ 86001, USA. [2]Department of Astronomy, Space Sciences Building, Cornell University, Ithaca, NY 14853, USA. [3]Department of Earth and Space Sciences, Washington University, St. Louis, MO 63130, USA. [4]Jet Propulsion Laboratory, California Institute of Technology, Pasadena, CA 91109, USA. [5]Center for Planetary Science, Danish Space Research Institute and Niels Bohr Institute for Astronomy, Physics, and Geophysics, University of Copenhagen, Denmark. [6]NASA Ames Research Center/SETI Institute, Moffett Field, CA 94035, USA. [7]Max Planck Institut für Aeronomie, Katlenburg-Lindau, D-37191, Germany. [8]Institute of Physics and Astronomy, Aarhus University, Aarhus, Denmark. [9]State University of New York, Department of Geosciences, Stony Brook, NY 11794, USA. [10]Department of Earth and Planetary Sciences, University of Tennessee, Knoxville, TN 37996, USA. [11]Arizona State University, Department of Geological Sciences, Tempe, AZ 85287, USA. [12]NASA Ames Research Center, Moffett Field, CA 94035, USA. [13]University of Arizona, Lunar and Planetary Laboratory, Tucson, AZ 85721, USA. [14]Department of Earth and Space Sciences and McDonnell Center for Space Sciences, Washington University, St. Louis, MO 63130, USA.

*To whom correspondence should be addressed. E-mail: kherkenhoff@usgs.gov

Fig. 1. MI image of soil target at Sugar Loaf Flats, showing partial annular imprint of Mössbauer contact plate. Contact plate was not parallel to soil surface, so contact was made only in the brighter part of the image. The part of MI full frame 2M1321-32632 shown here is 27 by 22 mm. Illumination from bottom.

Fig. 2. Merge of MI image 2M132842785 of feature Serpent (trenched), taken sol 073, with Pancam enhanced color data (602 nm, 535 nm, and 483 nm). Illumination from top; frame is 32 mm square.

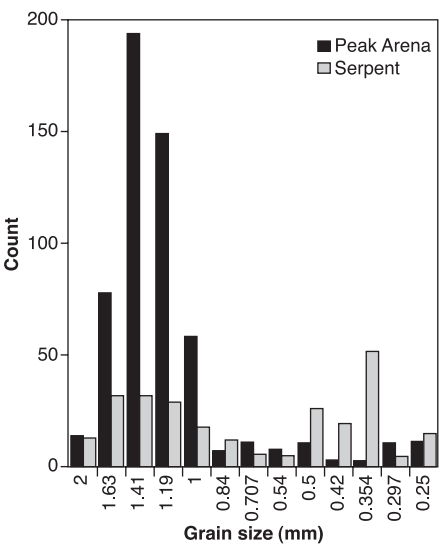

Fig. 3. Grain count versus size for bedform materials at Gusev crater, showing variation in modalities. Grain size increases from right to left. Data were gathered from images shown in figure 2 and figure 2C of (*20*).

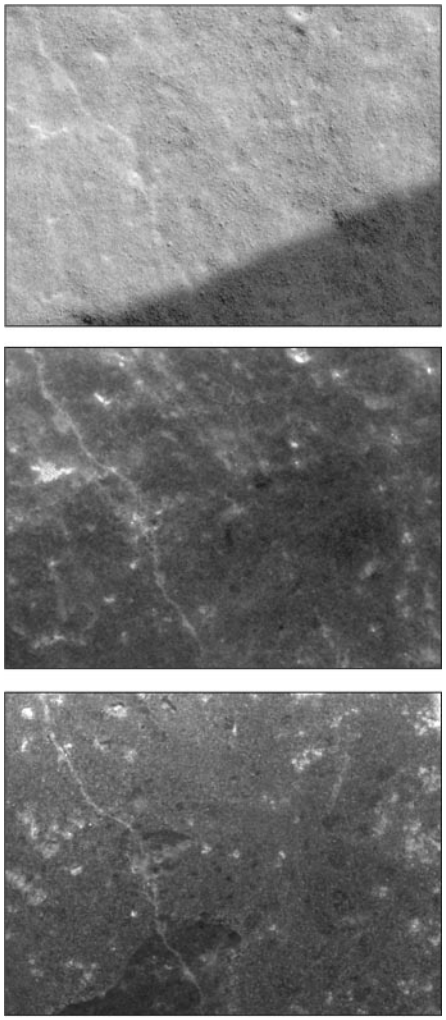

Fig. 4. MI images of rock called Adirondack. (**Top**) Part of image 2M127876442 showing natural surface. (**Middle**) Part of image 2M129296827 showing same area after RAT brushing. (**Bottom**) Part of image 2M129468568 showing same area after RAT grinding. Each subframe ~20 mm across. Illumination from top, shadow at lower right in left frame; right frames show surface in complete shadow.

sistent with electrostatic cohesion or minor cementation of dust grains (*15*). Some of the MI images of soil or dusty rocks show linear textures that may have been formed by recent winds.

MI data were used to quantify grain-size distribution and shape in soils and bedforms at Gusev Crater. Biases and sources of measurement errors in image analyses of terrestrial sediments have been studied and quantified (*16*–*18*) and are mainly related to the resolution of the instrument, the size of individual grains, and the light-scattering effect and projected shadows on grains. Representative areas of equal size in each MI image were selected for statistical data gathering, and grains were counted by several analysts. Longest and shortest axes of grains were measured with an average deviation of ±1 pixel (31 μm) (*18*). Single grains were identified with confidence when their diameter was at least 120 μm (~4 pixels). At this size, the error margin of ±1 pixel still represents a significant fraction of a grain size (~30%). Therefore, we limited our counts to grain diameters >210 μm, where confidence is high and error margin acceptable. Our results thus do not include the very fine sand to clay fractions. Grain-size classifications of the MI samples use the Wentworth scale (*19*).

Most of the soils at Gusev are composed of very fine grains or agglomerates of grains at the margin of MI resolution. Bedforms have coarser particles at their crests and finer grains in the troughs, like aeolian ripples on Earth (*20*). Particle-size frequencies of sampled ripple surfaces such as Arena (*20*, *21*) typically are bimodal, with one mode centered between 1 and 2 mm (coarse sand to very fine granules) and the other below 210 μm (fine to very fine sand). MI images of soil (e.g., Fig. 2) indicate that grains too small to be resolved are present, but statistics for grains smaller than 210 μm are not included in Fig. 3. The larger grains are rigid (as opposed to agglomerates of finer grains), based upon the lack of modification by the Mössbauer contact plate. The bedform Serpent, analyzed on sol 73, has a trimodal distribution, with an additional mode centered between 500 and 250 μm (Figs. 2 and 3). Specific shapes are associated with the coarser modes: granules are platy-rounded to ellipsoidal; medium sands are spherical. The shape of the finest sands at the margin of resolution could not be assessed. Typical soils include a mixture of grain sizes and larger clasts. Multimodalities in grain-size distribution are usually associated with multiple processes having affected the grains. In this case, the size and sphericity of the medium sand is consistent with aeolian processes (*20*), while the platy-rounded and ellipsoidal shapes of the granules are associated with aqueous or aeolian processes on Earth.

Rocks at the Gusev site were examined by the MI before and after brushing and grinding by the RAT (*12*) (Fig. 4 and Plates 12 and 13). The images of natural surfaces show a submillimeter texture that appears to be caused by cohesion of unresolved dust grains on the rocks, similar to the agglomerates seen in the soils at Gusev. Pits and veins are visible in the rocks before and after brushing or grinding, but only after dust has been removed from the rock surface can the color and reflectance of the veins be observed. MI observations of areas that have been abraded by the RAT reveal evidence for thin coatings on the rocks, which may be products of alteration by water (*22*). The images show mineral grains, probably phenocrysts, beneath the coatings. These observations are consistent with the rocks having a volcanic origin, as indicated by other Spirit observations (*23*).

References and Notes

1. K. E. Herkenhoff *et al*., *J. Geophys. Res*. **108**, 8065 (2003).
2. S. W. Squyres, *et al*., *J. Geophys. Res*. **108**, 8062 (2003).
3. J. F. Bell III *et al*., *J. Geophys. Res*. **108**, 8063 (2003).
4. J. N. Maki *et al*., *J. Geophys. Res*. **108**, 8071 (2003).
5. A martian solar day has a mean period of 24 hours 39 min 35.244 s and is referred to as a sol to distinguish it from a roughly 3% shorter solar day on Earth. A martian sidereal day, as measured with respect to the fixed stars, is 24 hours 37 min 22.663 s, as compared with 23 hours 56 min 04.0905 s for Earth. See www.giss.nasa.gov/tools/mars24 for more information.
6. The term martian soil is used here to denote any loose, unconsolidated materials that can be distinguished from rocks, bedrock, or strongly cohesive sediments. No implication of the presence or absence of organic materials or living matter is intended.
7. R. E. Arvidson *et al*., *Science* **305**, 821 (2004).
8. P. Bertelsen *et al*., *Science* **305**, 827 (2004).
9. S. W. Squyres *et al*., *Science* **305**, 794 (2004).
10. J. F. Bell III *et al*., *Science* **305**, 800 (2004).
11. R. V. Morris *et al*., *Science* **305**, 833 (2004).
12. S. Gorevan *et al*., *J. Geophys. Res*. **108**, 8068 (2003).
13. R. Gellert *et al*., *Science* **305**, 829 (2004).
14. The ability to resolve individual grains with the MI depends on the illumination of the scene and the contrast between the grain and its surroundings. Typically, an object must subtend at least 3 pixels to be recognized in an image.
15. G. Landis *et al*., in *Lunar and Planetary Science* **XXXV** (LPI Publication 1197, Lunar and Planetary Institute, Houston, CD-ROM, 2004).
16. J. B. Butler, S. N. Lane, J. H. Chandler, *J. Hydraulic Res*. **39**, 1 (2001).
17. D. M. Rubin, *J. Sed. Res*. **74**, 160 (2004).
18. We used NIH Image, version 1.63 (*24*).
19. C. K. Wentworth, *J. Geol*. **30**, 377 (1922).
20. R. Greeley *et al*., *Science* **305**, 810 (2004).
21. Names have been assigned to areographic features by the Mars Exploration Rover (MER) team for planning and operations purposes. The names are not formally recognized by the International Astronomical Union.
22. H. Y. McSween *et al*., *Science* **305**, 842 (2004).
23. P. R. Christensen *et al*., *Science* **305**, 837 (2004).
24. J. Wagner *et al*., in preparation.
25. The U.S. Geological Survey MER Team developed MI software and created various data products, including some of those displayed in this issue: B. Archinal, J. Barrett, K. Becker, T. Becker, D. Burr, D. Cook, T. Hare, A. Howington-Kraus, R. Kirk, E. Lee, M. Rosiek, B. Sucharski, T. Sucharski, and J. Torson (project engineer). The Ames MER team and Mark Lemmon developed software to merge focal sections and generate anaglyphs from them. The MER Rover Planners provided excellent support of the MI investigation by commanding the arm and MI dust cover. Reviews of this paper by M. Chapman, L. Keszthelyi, S. Thompson, C. Weitz, and four anonymous referees are much appreciated. The work described here was supported by the NASA Jet Propulsion Laboratory Mars Exploration Rover project. The use of trade, product, or firm names in this paper does not imply endorsement by the U. S. government.

Plates Referenced in Article

www.sciencemag.org/cgi/content/full/305/5685/824/DC1
Plates 12 and 13

6 May 2004; accepted 15 July 2004